

# LEAPER: Modeling Cloud FPGA-based Systems via Transfer Learning

Gagandeep Singh<sup>a</sup>

Dionysios Diamantopoulos<sup>b</sup>

Juan Gómez-Luna<sup>a</sup>

Sander Stuijk<sup>c</sup>

Henk Corporaal<sup>c</sup>

Onur Mutlu<sup>a</sup>

<sup>a</sup>ETH Zürich

<sup>b</sup>IBM Research Europe, Zurich

<sup>c</sup>Eindhoven University of Technology

**Abstract**—Machine-learning-based models have recently gained traction as a way to overcome the slow downstream implementation process of FPGAs by building models that provide fast and accurate performance predictions. However, these models suffer from two main limitations: (1) training requires large amounts of data (features extracted from FPGA synthesis and implementation reports), which is cost-inefficient because of the time-consuming FPGA design cycle; (2) a model trained for a specific environment cannot predict for a new, unknown environment. In a cloud system, where getting access to platforms is typically costly, data collection for ML models can significantly increase the total-cost-ownership (TCO) of a system. To overcome these limitations, we propose LEAPER, a *transfer learning*-based approach for FPGA-based systems that adapts an existing ML-based model to a new, unknown environment to provide fast and accurate performance and resource utilization predictions. Experimental results show that our approach delivers, on average, 85% accuracy when we use our transferred model for prediction in a cloud environment with *5-shot learning* and reduces design-space exploration time by 10×, from days to only a few hours.

**Index Terms**—Cloud computing, FPGAs, machine learning, transfer learning, reconfigurable computing

## I. INTRODUCTION

The need for energy efficiency from edge to cloud computing has boosted the widespread adoption of FPGAs. In addition to the reconfigurability of an FPGA to implement diverse workloads, FPGA’s flexibility in a cloud system is attributed to its cloud deployment model [1]–[12]. These deployment models span from on-premises clusters to compute, storage, and networking capacity in public clouds.

An FPGA is highly configurable as its circuitry can be tailored to perform any task. The large configuration space of FPGA and the complex interactions among configuration options lead many developers to explore individual optimization options in an ad-hoc manner [13], [14]. Moreover, FPGAs have infamously low productivity due to the time-consuming FPGA implementation process [15]. A common challenge that past works have faced is how to evaluate the performance of an FPGA implementation in a reasonable amount of time [16]. To overcome this problem, researchers have recently employed machine learning (ML)-based models [16]–[25] to estimate the performance of an FPGA-based system quickly. These models are based, in turn, on traditional ML approaches. Traditional ML models have three fundamental issues that can reduce the usability for assessing FPGA performance, especially in a cloud system.

First, they are trained for specific workloads, fixed hardware, and/or a set of inputs. Therefore, when presented with a different feature-space distribution because of a new workload or hardware, an ML model must be retrained from scratch. Otherwise, the model will perform poorly because the trained model does not have a notion of the new, unknown environment<sup>1</sup>. Therefore, traditional ML-based models have limited *re-usability*.

Second, learning-based approaches, such as neural networks, require a considerable number of samples to construct a useful prediction model. Collecting such a large number of samples is often slow and time-consuming due to the very long FPGA implementation cycle. Similarly, in

cloud computing or other settings, where getting access to platforms is typically *costly* and *error-prone*, which makes collecting enough samples almost *infeasible*.

Third, traditional machine learning with limited samples is prone to serious *overfitting* problems (i.e., when a model matches too closely to the training data) [26], limiting model generalization.

Figure 1 demonstrates the traditional approach to building ML-based models. Using the traditional approach, we would need to create two separate prediction models, one for the low-end edge environment and another one for the high-end cloud environment, each one requiring a large number of samples.

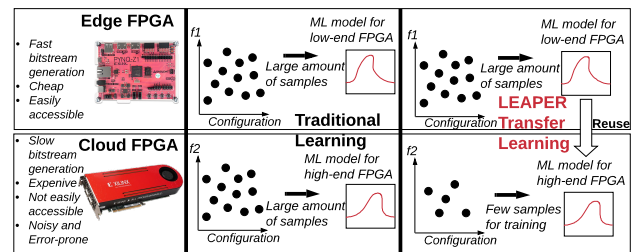


**Fig. 1:** Comparison of traditional learning approach and LEAPER.

**Our goal** is to leverage an ML-based performance model trained on a low-end local system to: (1) predict the performance in a new, unknown, high-end FPGA-based system, (2) predict the performance of a new, unknown application to overcome the limitations of current ML-based performance models in a cloud environment.

To this end, we present LEAPER<sup>2</sup>, a transfer learning-based model that predicts performance of a new, unknown high-end FPGA-based system. First, we train LEAPER on a low-end local system see Figure 2. Second, LEAPER uses predictive modeling to train a *base ML-based model* on the local system, and statistical techniques to collect representative training data efficiently. Third, LEAPER uses *transfer learning* [27] to efficiently adapt the trained base model to an unknown, *target* environment (i.e., a high-end system) with a few samples from the target environment as possible. LEAPER also transfers models across unknown, new applications.

This paradigm is also referred to as *few-shot learning* [28]. The idea behind few-shot learning is that, similar to humans, algorithms can learn from past experiences and transfer the knowledge to accomplish previously-unknown tasks more efficiently. The transferred models usually have high generality [28].

In this paper, we make the following contributions:

- 1) We present the first use of *few-shot learning* to transfer FPGA-based computing models across different hardware platforms and applications (Section II). This approach dramatically reduces (up to 10×) the training overhead by adapting a *base model*, trained on a low-end edge FPGA platform to a new, unknown high-end environment (a cloud environment in our

<sup>2</sup>We call our mechanism LEAPER because it allows us to hop or “leap” between machine learning models.

<sup>1</sup>We consider a new workload or hardware as an environment.)

case) rather than building a new model from scratch (Section III-C).

- 2) Unlike state-of-the-art works [16]–[22] in FPGA modeling that use deep neural networks, we show that classic machine learning models based on decision tree algorithms are enough to build an accurate FPGA performance prediction model.
- 3) We demonstrate our approach across *five* state-of-the-art, high-end, on-premise cloud FPGA-based platforms with *three* different interconnect technologies on *six* real-world applications (Section III). For *5-shot* learning, we achieve an average performance and area prediction accuracy of 80–90%.

## II. LEAPER

LEAPER is a performance and resource estimation approach to *transfer* ML models based on classic machine learning algorithms [29], [30] across different FPGA-based platforms and across different applications on the same platform. First, we give an overview of LEAPER (Section II-A). Second, we describe FPGA-based accelerator configuration options and application features used for training our base model (Section II-B). Third, we briefly describe the base model training (Section II-C). Fourth, we explain the key component of LEAPER: the transfer learning technique (Section II-D).

### A. Overview

Figure 2 depicts the key components of LEAPER. The upper part of the figure describes the base model building, while the lower part shows the target model building.

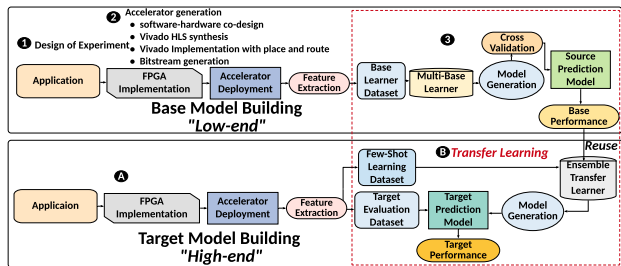


Fig. 2: Overview of LEAPER.

**Base Model Building.** LEAPER’s base model building consists of three phases. In the first phase (1 in Figure 2), we employ the *design of experiment* (DoE) technique [31] to select a small set of input configurations that well represent the entire space of input configurations ( $c_{doe}$ ) to build a highly accurate *base learner*. By using DoE, we minimize the number of experiments needed to gather training data for LEAPER while ensuring good quality training data. In the second phase (2), FPGA implementations are made with a software-hardware co-design process. Once the FPGA design has been implemented, the resulting FPGA-based accelerator is deployed in a system with a host CPU. Then, we run the  $c_{doe}$  configurations on the deployed FPGA-based system to gather samples for training our base model. The generated responses, along with the applied configuration options (*ref.* Table I), form the input to our base ML algorithm. In the third phase (3), we train our ML algorithm (Section II-C) using ensemble learning [32]. During this phase, we perform 10-fold cross-validation to validate the performance of our model. During cross-validation, we divide our dataset into 10 equal subsamples of which 1 set is used for validation. Once trained, the framework can predict the performance and resource usage on the base system (a low-end FPGA) of previously-unseen configurations, which are not part of the  $c_{doe}$  configurations used during the training.

**Target Model Building.** We use transfer learning to reuse an ML model (trained on a low-end FPGA) in a high-end cloud environment. The first phase (A in Figure 2) of the target model building, we repeat the accelerator generation

TABLE I: The FPGA configuration options used to train our ML-models.

| Configuration      | Description   |
|--------------------|---|
| Pipelining (PL)    | Enabled/Disabled  |
| Partitioning (PR)  | Block/Cyclic/Complete (Factor: $2^n, 1 \leq n \leq 6$ ) |
| Inlining (I)       | Enabled/Disabled function inlining                      |
| Dataflow (D)       | Task level pipelining                                   |
| Read burst (R)     | Read data burst from the host                           |
| Write burst (W)    | Write data burst from the host                          |
| Unrolling (U)      | Unrolling factor (Factor: $2^n, 1 \leq n \leq 6$ )      |
| FPGA Frequency (F) | Four-different frequency levels for the FPGA logic      |

step to get a few samples<sup>3</sup> We perform this step to create our *few-shot* learning dataset ( $c_{fl}$ ), which is used to adapt the base model to the target cloud environment. In the final phase (B), we train our transfer learners (see Section II-D) to leverage the base model to perform predictions for a new, unknown target environment (new application or hardware).

### B. FPGA Configuration Options and Application Features

The ML feature vector used for training an ML model is composed of FPGA configuration options (Table I) and application features (Table II).

**FPGA Configuration Options.** Table I describes commonly used high-level synthesis (HLS) [33] pragmas that belong to our FPGA configuration options, for both the base and the target environment, and constitute part of our ML feature vector. We select these HLS pragmas because they are used to optimize and tune the performance of FPGA implementations [34].

We include these configuration options among the features because of their large potential impact on performance. Both *loop pipelining* (PL) and *loop unrolling* (U) can improve application performance significantly. To enable simultaneous memory accesses, *array partitioning* (PR) divides arrays into smaller memory units of arbitrary dimensions to map them to different memory banks. This optimization produces considerable speedups but consumes more resources. *Inlining* (I) ensures that a function is instantiated as dedicated hardware. *Dataflow* (D) allows parallel execution of tasks. In addition, *burst read* (R) and *burst write* (W) access to/from the host guarantee that the accelerator is not stalled for data. Moreover, *FPGA frequency* (F) affects not only performance but also resource consumption. For instance, to meet the FPGA timing requirements, the FPGA tool tries to insert registers between the flip-flops, which increases resource consumption. The actual configuration space of an application depends on the specific application characteristics (see Table III). For example, we include loop unrolling in the configuration space when an application contains loops that can be unrolled. In total, our configuration options for a particular application consist of up to 4,608 configurations.

**Application Features.** We also include inherent application features in our training dataset. For each application kernel  $k$  processing a dataset  $d$ , we obtain an application profile  $p(k, d)$ .  $p(k, d)$  is a vector where each parameter is a statistic about an application feature. Table II lists the main application features we extract by using the LLVM-based PISA analysis tool [35]. Ultimately, the application profile  $p$  has 395 features, which includes all the sub-features of each metric we consider. We perform feature selection to select the 100 most important features to analyze the behavior of an application with the FPGA configuration options (see Table I).

### C. Base Model Building

The third phase of the base model building is the base learner training phase. Formally, in a learning task,  $\mathcal{X}$  represents feature space with label  $\mathcal{Y}$ , where a machine learning model is responsible for estimating a

<sup>3</sup>We show by our experiments (Section III) that up to 5 samples are enough to learn the distribution of a new environment.

**TABLE II:** Main application features extracted from LLVM.

| Application Feature             | Description   |
|---------------------------------|---|
| Instruction Mix                 | Fraction of instruction types (integer, floating point, memory read, memory write, etc.)  |
| ILP                             | Instruction-level parallelism on an ideal machine.  |
| Data/Instruction Reuse Distance | For a given distance $\delta$ , probability of reusing one data element/instruction (in a certain memory location) before accessing $\delta$ other unique data elements/instructions (in different memory locations). |
| Register Traffic                | Average number of registers per instruction.  |
| Memory Footprint                | Total memory size used by the application.  |

function  $f : \mathcal{X} \rightarrow \mathcal{Y}$ . LEAPER predicts the execution time (resource consumption)  $\mathcal{Y}$  for a tuple  $(p, k, c)$  that belongs to the ML feature space  $\mathcal{X}$ , where  $p$  is an FPGA-based configuration options (ref. Section II-B) that runs an application characteristics  $k$ , with an optimization configuration vector  $c$ .

We use an *ensemble* of two base learners. Our base learners are nonlinear algorithms that can capture the intricacies of FPGA architectures by predicting the execution time or resource consumption. Our first algorithm is the *random forest* (RF) [30], which is based on *bagging* [36]. We use RF to avoid a complex feature-selection scheme since RF embeds automatic procedures that are able to screen many input features [37], like the ones we selected in the previous section. Starting from a root node, RF constructs a tree and iteratively grows the tree by associating a node with a splitting value for an input feature to generate two child nodes. Each node is associated with a prediction of the target metric equal to the observed mean value in the training dataset for the input subspace that the node represents. Our second learner is *gradient boosting* [38]. Bagging [39] reduces model variance, and boosting decreases errors [40]. Therefore, we use RF and gradient boosting together to increase the predictive power of our final trained base model.

The training dataset for our base model has two parts: (1) an optimization configuration vector  $c$ , whose representation remains invariant across different environments, and (2) the responses corresponding to each tuple  $(p, k, c)$ . To gather the architectural responses, we run each application  $k$  belonging to the training set  $\mathbb{T}$  with an input dataset  $d$  on an FPGA-based platform  $p$ , deploying a configuration  $c$ . This way, we obtain the execution time for the tuple  $(p, k, d)$ , which we can use as a *label* ( $\mathcal{Y}$ ) for training our base learner for performance prediction. We build a similar model to predict resource consumption, where we use the resource consumption ( $\eta_{\{BRAM, FF, LUT, DSP\}}$ ) of the tuple  $(p, k, d)$  as a *label* when we train our base learner for resource consumption. After training our base learners, we can predict the execution time (resource usage) ( $\hat{f}_s : \mathcal{X}_s \rightarrow \mathcal{Y}_s$ ) of tuples  $(p, k, d)$  that are *not* in the training set. We use 10-fold cross-validation to validate our base learner’s performance, whereby the data is divided into ten validation sets.

#### D. Cloud Model Building via Transfer Learner

LEAPER provides the ability to transfer trained FPGA models across different environments. LEAPER defines a target environment  $\tau_t$  as an environment for which we wish to build a prediction model  $\hat{f}_t$  where, however, data collection is expensive, and a source environment  $\tau_s$  as an environment for which we can *cheaply* collect many samples to build an ML model  $f_s$ . In our case,  $\tau_s$  is a low-cost edge FPGA, while  $\tau_t$  is a high-cost cloud FPGA. LEAPER then transfers the ML model for  $\tau_s$  to  $\tau_t$ .

Algorithm 1 presents LEAPER’s transfer learning approach. We use a few sample observations  $c_{tl}$  (line 3) from both the source and the target environments to make our transfer learners (TLs) learn how to make source environment distribution to target environment distribution.

$c_{tl}$  is a subset of  $c_{doe}$ . This helps us to avoid measuring all  $c_{doe}$  from a cost-prohibitive target cloud environment. LEAPER trains TLs (line 4) that transform the source performance and utilization model  $f_s$  to the target model  $\hat{f}_t$ .

#### Algorithm 1: LEAPER’s transfer learning

---

**Input:** (1) Base learner ( $f_s$ ) i.e., trained low-end edge FPGA prediction model,  
(2) Sub-sampled *few-shot learning* dataset  $c_{tl} \subset c_{doe}$  from the base and the target model

**Output:** Target cloud FPGA model  $\hat{f}_t : \mathcal{X}_t \rightarrow \mathcal{Y}_t$

- 1 initialization: Maximum number of iterations  $M$
- 2 **while**  $M \neq 0$  **do**
- 3     Normalize the feature vector
- 4     Train ensemble transfer learners (TL) with  $c_{tl}$
- 5     Find the candidate TL ( $\hat{f}_t$ ):
- 6          $\hat{h}_t : \mathcal{X}_{tl} \rightarrow \mathcal{Y}_{tl}$  that minimizes the error over the  $c_{doe} - c_{tl}$
- 7     Compute the mean relative error:
$$\epsilon_{mre} = \frac{1}{c_{doe} - c_{tl}} \sum_{i=1}^{c_{doe} - c_{tl}} \frac{|y_t^{acc} - y_t^{pred}|}{y_t^{acc}}$$
- 8     Use identified  $\hat{h}_t$  to transform predictions of  $f_s$
- 9     :
- 10          $\hat{f}_t = \hat{h}_t(f_s)$                                      where
- 11          $f_s : \mathcal{X}_s \rightarrow \mathcal{Y}_s$
- 11          $M \leftarrow M - 1$
- 12 **end**
- 13 **return**  $\hat{f}_t$

---

In transfer learning, a weak relationship between the base and the target environment can decrease the predictive power of the target environment model. This degradation is referred to as a *negative transfer* [41]. To avoid this, we use an ensemble model trained on the transfer set (i.e., the *few-shot learning* dataset in Figure 2) as our transfer learners (TLs). We chose these specific TL methods based on our extensive empirical analysis. Our first TL is based on TrAdaBoost [26], a boosting algorithm, which is a learning framework that fuses many weak learners into one strong predictor by adjusting the weights of training instances. The motivation behind such an approach is that by fusing many weak learners boosting can improve the overall predictions in areas where the previously grown learners did not perform well. We use Gaussian process regression [42] as our second TL. It is a Bayesian non-parametric algorithm that calculates the probability distribution over all the appropriate functions that fit the data. To transfer a trained model, we train TrAdaBoost and Gaussian process regression, which are our candidate TLs. We choose the one that has minimum transfer error (ref. Line 6).

By using the selected  $c_{tl}$ , we generate a transfer model  $\hat{h}_t$  that provides the lowest mean relative error (line 7). Finally, to build  $\hat{f}_t$  from  $f_s$  we use  $\hat{h}_t$ , which performs a non-linear transformation of the predictions of  $f_s$ . We use a non-linear transfer learner because, based on our analysis (Section III-E), non-linear models are able to capture the nonlinearity present in the FPGA performance and configuration options.

### III. EVALUATION

We evaluate LEAPER using six benchmarks (see Table III), which are hand-tuned for FPGA execution covering several application domains, i.e., (1) **image processing**: histogram calculation (*hist*) [43], and canny

**TABLE III:** Evaluated application description including their major kernels and the input dataset. For major kernels, we mention the optimization space where  $\times$  represents the optimization being applied to multiple loops or elements. *ref.* Table I for description of the optimization options.

| Application | Domain           | Major Kernels  | Dataset                               | Optimization space  |
|-------------|------------------|--|---------------------------------------|---|
| blstm [44]  | Machine learning | Hidden layer fw<br>Hidden layer back<br>Output layer                       | Fraktur OCR [47]                      | $2 \times \text{PL}, 3 \times \text{PR}(2,4), \text{I}, 2 \times \text{U}$<br>$2 \times \text{PL}, \text{I}, 2 \times \text{U}$<br>$\text{PL}, \text{I}, \text{U}+\text{D}, \text{R}, \text{W}, \text{F}$                       |
| cedd [43]   | Image proc.      | Gaussian filter<br>Sobel filter<br>Suppression filter<br>Hysteresis filter | Frame-354 $\times$ 626<br>1000 frames | $\text{PL}, \text{PR}(2,4), \text{I}, \text{U}$<br>$\text{PL}, \text{PR}(2,4), \text{I}, \text{U}$<br>$\text{PL}, \text{PR}(2,4), \text{I}, \text{U}$<br>$\text{PL}, \text{I}, \text{U}+\text{D}, \text{R}, \text{W}, \text{F}$ |
| digit [45]  | Machine learning | Hamming dist.<br>KNN voting  | MNIST-18000 train<br>2000 test        | $2 \times \text{PL}, 3 \times \text{PR}(2,4), \text{I}, 4 \times \text{U}$<br>$\text{I}+\text{R}, \text{W}, \text{F}$   |
| hist [43]   | Image proc.      | Histogram avg.   | Input-1536 $\times$ 1024<br>Bins-256  | $\text{PL}, \text{PR}(\text{all}), \text{I}, \text{D},$<br>$\text{R}, \text{W}, \text{U}, \text{F}$   |
| select [43] | Database         | Selection  | 1048576 elements                      | $\text{PL}, \text{I}, \text{D}, \text{R}, \text{W}, \text{F}$   |
| sc [43]     | Data reorg.      | Count<br>Compact   | 1048576 elements                      | $\text{PL}, \text{I}, \text{D}, \text{R}, \text{W}, \text{U}, \text{F}$   |

**TABLE IV:** System parameters and configuration.

| Low-end base system   |                               |                    | Indicative price             |
|---|-------------------------------|--------------------|------------------------------|
| <b>Embedded Board</b>   | PYNQ-Z1 ZYNQ [48]             | XC7Z020-1CLG400C   | \$199 <sup>4</sup>           |
| ARM Cortex-A9 processor @650MHz, dual-core  |                               |                    |                              |
| <b>On-prem cloud target system with OpenStack [50] and KVM Hypervisor</b>                   |                               |                    |                              |
| <b>Host Configuration</b>   | IBM <sup>®</sup> POWER9 AC922 | @2.3 GHz, 16 cores | \$55000-\$75000 <sup>5</sup> |
| 4-way SMT, 32 KiB L1 cache, 256 KiB L2 cache,<br>10 MiB L3 cache, 32GiB RDIMM DDR4 2666 MHz |                               |                    |                              |
| <b>FPGA Description</b>   |                               |                    |                              |
| <b>Board</b>  | <b>FPGA Family</b>            | <b>Device</b>      | <b>Interface</b>             |
| ADM-PCIE-8K5 [51]   | Kintex UltraScale             | XCKU115-2          | CAPI-1                       |
| ADM-PCIE-KU3 [52]   | Kintex UltraScale             | XCKU060-2          | CAPI-1                       |
| Semptian NSA241 [53]  | Virtex UltraScale             | XCVU9P-2           | CAPI-2                       |
| ADM-PCIE-9V3 [54]   | Virtex UltraScale             | XCVU3P-2           | CAPI-2                       |
| N250SP [55]   | Kintex UltraScale             | KU15P-2            | CAPI-2                       |

<sup>4</sup> <https://store.digilentinc.com/pynq-z1-python-productivity-for-zynq-7000-arm-fpga-soc/>

<sup>5</sup> <https://www.microway.com/product/ibm-power-systems-ac922/>

N/A: Not available indicative price from an online store, but in the region of \$2500-\$5000 for our purchased on-prem cards.

edge detection (*cedd*) [43]; **(2) machine learning:** binary long short term memory (*blstm*) [44], digit recognition (*digit*) [45]; **(3) databases:** relational operation (*select*) [46]; and **(4) data reorganization:** stream compaction (*sc*) [43]. These kernels are specified in C/C++ code using high-level synthesis (HLS) that is compiled to the FPGA target.

#### A. Hardware Platform and Tools

Table IV summarizes the system details of the source and our on-prem research cloud environment. We select a *low-end* edge PYNQ-Z1 [48] as the source platform to build base learners. We use the Accelerator Coherency Port (ACP) port [49] for attaching accelerators to the ARM Cortex A9 CPU of PYNQ-Z1. Figure 3a shows the target cloud environment platform with a host system connected to an FPGA board.

For accelerator implementation and deployment, we leverage CAPI-compatible tools offered by Xilinx. In particular, we use the Xilinx SDSoc [56] design tool for implementing the low-end system  $\tau_s$  and the Vivado HLS [33] with IBM<sup>6</sup> CAPI-SNAP framework<sup>7</sup> for the high-end system  $\tau_t$ . The SNAP framework provides seamless integration of an accelerator [57] and allows to exchange of control signals between the host and the FPGA processing elements over the AXI lite interface [58]. On task completion, the processing element notifies the host system via the AXI lite interface and transfers back the results via CAPI-supported DMA transactions. As derived from the indicative prices listed in the right column of Table IV, the total cost of ownership (TCO) of a high-end system can be more than 100x of that of the low-end one,

<sup>6</sup>IBM and POWER9 are registered trademarks or common law marks of International Business Machines Corp., registered in many jurisdictions worldwide. Other product and service names might be trademarks of IBM or other companies.

<sup>7</sup><https://github.com/open-power/snap>

and thus it can be prohibitive for a bare-metal deployment for many users. Complementary, moving a workload to a cloud FPGA instance should offer such a speedup that it compensates for the extra design time, effort, and cost of this decision by the end-user. LEAPER helps a user to rapidly quantify such a decision by experimenting with low-cost and broadly available FPGAs, like the PYNQ-Z1.

#### B. Target Model Accuracy Analysis

LEAPER is used to transfer a trained model using *few-shot learning* to the  $\tau_t$ 's optimization space. We then analyze the accuracy of the newly-built target model to predict the performance and resource utilization of all the other configurations in  $\tau_t$ . We evaluate the accuracy of the transferred model in terms of the relative error ( $\epsilon_i$ ) to indicate the proximity of the predicted value  $y'_i$  to the actual value  $y_i$  across  $N$  test samples. The mean relative error (MRE) is calculated with Equation 1.

$$MRE = \frac{1}{N} \sum_{i=1}^N \epsilon_i = \frac{1}{N} \sum_{i=1}^N \frac{|y'_i - y_i|}{y_i}. \quad (1)$$

**Performance Model Transfer.** Figure 4 shows LEAPER's accuracy for transferring *across different cloud platforms*. We make the following four observations. First, as we increase the number of labeled samples, the target model accuracy increases. However, the accuracy saturates and, with 5-10 *shots*, we can achieve an accuracy as high as 80 to 90%. Second, compared to applications with multiple complex kernels (*blstm*, *cedd*, *digit*), simpler kernels (*hist*, *sc*, *select*) can be more easily transferred using fewer samples. Applications with multiple kernels have a larger optimization space. The large optimization space leads to more complex interactions that have compounding effects with other optimization options because we are modeling for multiple kernels rather than just a single kernel. Additionally, simple kernels such as *sc* and *select* have been implemented using *hls stream* interfaces. Here rather than storing intermediate data in local FPGA memories, we read streams of data, and hence certain complex optimizations (like array partitioning) cannot be applied. This leads to a change in the feature space of different environments. Third, less severe changes are more amenable to transfer as the source, and target models are more closely related, e.g., transferring to CAPI1 (PCIe Gen3 with  $\sim 3.3$  GB/s bandwidth) from low-end PYNQ with PCIe Gen2  $\sim 1.2$  GB/s bandwidth entails a smaller increment in bandwidth than moving to CAPI2, which offers R/W bandwidth of  $\sim 12.3$  GB/s. Fourth, change in the technology node from one FPGA to another (e.g., changing from ADMKU3 board to AD9V3 board) has a lower impact than changing the external bandwidth to a new interconnect standard on the transferring process.

Figure 5 shows LEAPER's accuracy for transferring ML models *across different applications*. First, we make a similar observation in the case of transferring models across different platforms: as we increase the number of training samples, the mean relative error for most applications decreases. Second, we notice that the most considerable improvement in accuracy occurs when our sample size ( $c_{ti}$ ) is between 2 to 10. In most cases, the accuracy saturates after 20 samples. Third, in some cases, we see a decrease in accuracy when increasing the number of samples. This result could be attributed to training with a small amount of data, which can sometimes lead to overfitting [26].

In Section III-E, we further explain our results by measuring the divergence of performance distributions to quantify the statistical distance between the source and target models.

**Resource Model Transfer.** By using LEAPER, we can also train a resource consumption model on a *low-end* source environment and transfer it to a high-end cloud

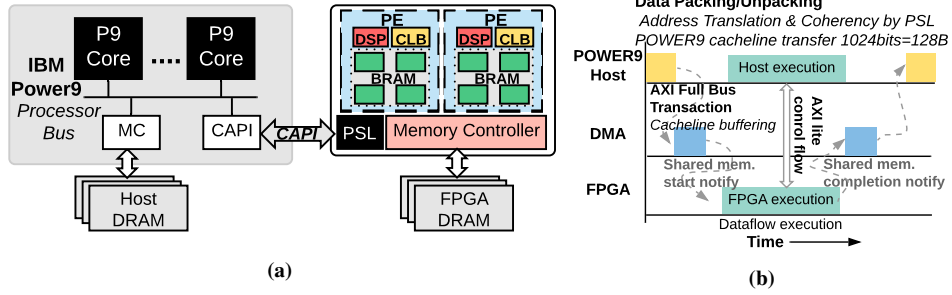


**Fig. 3:** (a) Experimental Cloud Platform: High-end on-prem cloud FPGA platform with IBM® POWER9 CPU (b) Execution timeline with data flow sequence from the host DRAM to the onboard FPGA memory.

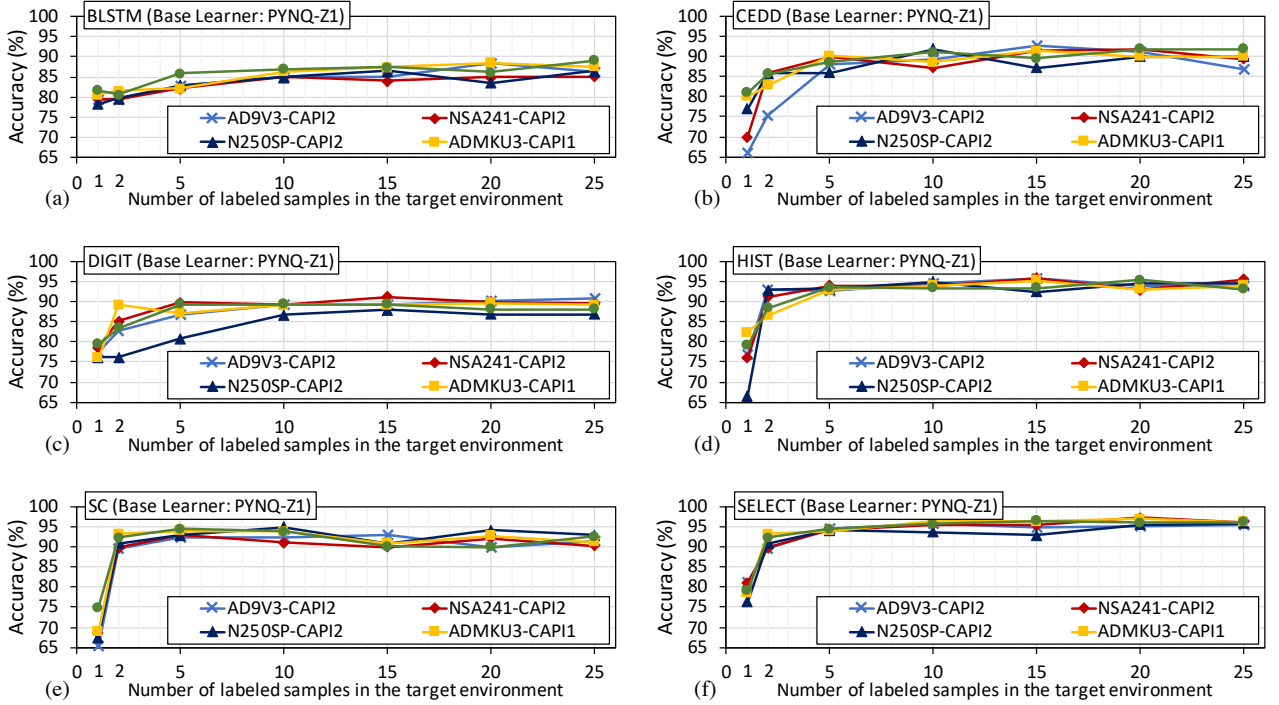


**Fig. 4:** LEAPER’s accuracy for transferring base models across CAPI-enabled cloud FPGA-based systems. The legends indicate the target platforms. The base model was trained on a low-end PYNQ-Z1 board and, for each application, we *transfer* this model to different high-end cloud FPGA-based platforms using different samples (horizontal axis) from the target platform.

target environment. Figure 6 shows the accuracy of a target model trained by *5-shot* transfer learning for predicting a resource utilization vector  $\eta_{\{BRAM, FF, LUT, DSP\}}$ . The reported accuracy is for the transferred model, i.e., using a base model (low-end FPGA) to predict a target model (high-end cloud FPGA) after few-shot learning. In Figure 6a, the horizontal axis depicts the target platform, while the base learner is trained on a PYNQ-Z1 board. In the case of an application model transfer (Figure 6b), the platform remains unchanged (PYNQ-Z1), while the base learner application changes (horizontal axis). We make three observations. First, the resource model shows low error rates for predicting BRAM and DSP. This is attributed to the fact that the technological configuration of these resources remains relatively unchanged across platforms (e.g., BRAM is implemented as 18 Kbits in both the source and target platforms). Second, flip-flops and look-up-tables have comparably higher error rates because the configuration of CLB<sup>8</sup> slices varies with the transistor technology and FPGA family. Third, Figure 6b shows the mean accuracy for transferring different application-based models on a fixed FPGA board.

We observe relatively low accuracy for DSP consumption while transferring a base model trained on *hist*. This low accuracy is because the *hist* FPGA implementation

<sup>8</sup>A configurable logic block (CLB) is the fundamental component of an FPGA, made up of look-up-tables (LUTs) and flip-flops (FF).

**TABLE V:** Average accuracy (%) comparison of LEAPER with decision tree (DT) and adaBoost (ADA) as TL for *5-shot* transfer.

| Environment        | DT   | ADA  | LEAPER |
|--------------------|------|------|--------|
| Across Board       | 77.7 | 83.2 | 89.8   |
| Across Application | 70.6 | 73.5 | 81.2   |

does not make use of DSP units. However, all other applications utilize DSPs. Therefore, the ML model trained on *hist* is not able to perform well in other *transferred* environments. Table V compares the average accuracy across different boards and applications using two different TLs: (1) decision tree (DT) [59], and (2) adaBoost (ADA) [60]. We observe that our ensemble of TLs are able to outperform both DT and ADA.

### C. Target Cloud FPGA Model Building Cost

Table VI shows the time for collecting (see “DoE run (hours)”) the 50 sampled DoE configurations ( $c_{l_{h,s}}$ ) that we use to gather training data. Please note that while the process of synthesis and P&R of the high-end system’s FPGA, which is needed to obtain the maximum operating clock frequency and the resources’ utilization, can be carried out offline, most of the cloud providers are offering VMs with all the appropriate software, IPs and licenses needed to generate an FPGA image ready to be deployed at their cloud infrastructure (e.g., the Vivado AMI of AWS [61]). This justifies the argument of the cost of the

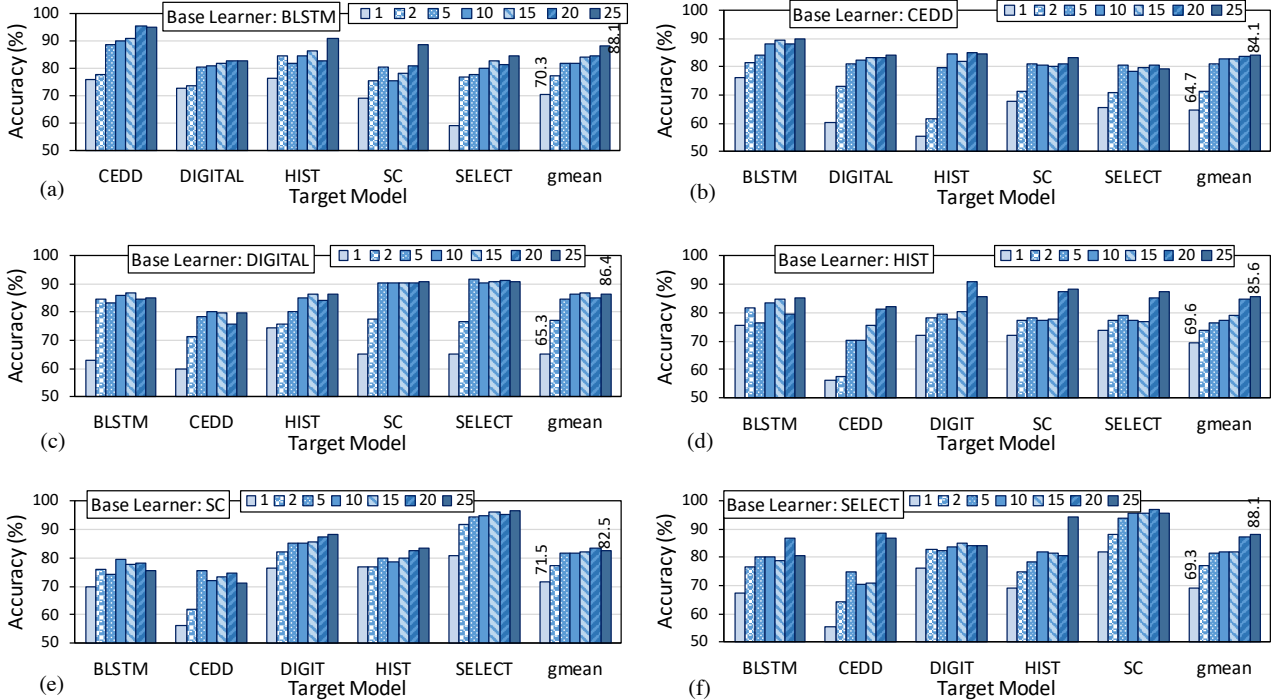


**Fig. 5:** LEAPER’s accuracy for transferring base models across various applications. The legends indicate the number of samples. Each plot represents a different application as a base learner. We *transfer* these base learners, trained on the PYNQ-Z1 platform, by using invariant configuration features to build a target application model.

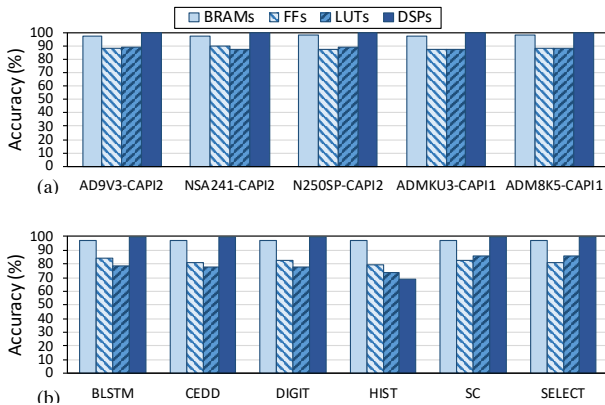


**Fig. 6:** LEAPER’s average accuracy for transferring FPGA resource usage models through *5-shot* using (a) a base learner trained on a low-end PYNQ-Z1 to different high-end target FPGA boards (horizontal axis), and (b) different applications as base learners (horizontal axis) to all the target applications, on low-end PYNQ-Z1 board.

cloud environment for DoE runs. We use a Linux image with FPGA and SoC development tools, IPs, and licences to generate bitstreams for the selected Xilinx devices in Table IV on the Nimbix cloud. Table VI also includes the execution time on the ADM-PCIE-KU3 cloud platform (“Exec (msec)”) and the transfer time (“Transfer (msec)”) for each model. By using transfer learning, the DoE runtime is amortized and, by using a few labeled samples  $c_{tl}$  (“*5-shot* (hours)”) from the target platform, we can transfer a previously trained model and make predictions for all the other configurations for the target platform. As a result, quick exploration and significant time savings (at least  $10.2\times$ ) are possible when transferring a model (i.e., “*5-shot* (hours)”) + “Transfer (msec)”) as compared to building a new model from scratch (i.e., “DoE run (hours)”) + “Exec (msec)”). Note, DoE reduces training samples from 500+ to 50, while *5-shot* transfer learning further reduces this space to 5, so we achieve  $100\times$

**TABLE VI:** DoE time for gathering sampled data points for a single CPU-FPGA platform (“DoE run (hours)”), DoE execution time on the deployed platform (“Exec (ms)”), Estimated Cost on a cloud platform (“Est. Cost (\$)”), time for gathering 5 labeled samples (“*5-shot* (hours)”), LEAPER time including the transfer time (“Transfer (msec)”), “Speedup” over building a new model from scratch using just the DoE data (still more cost-efficient than traditional “brute-force” training).

| Application Name | Transfer Time   |             |                            |                       |                 |                            |         |
|------------------|-----------------|-------------|----------------------------|-----------------------|-----------------|----------------------------|---------|
|                  | DoE run (hours) | Exec (msec) | Est.Cost <sup>7</sup> (\$) | <i>5-shot</i> (hours) | Transfer (msec) | Est.Cost <sup>7</sup> (\$) | Speedup |
| blstm            | 135             | 455         | 168.7                      | 13                    | 55.6            | 16.2                       | 10.4    |
| cedd             | 124             | 295         | 155.0                      | 12                    | 26.5            | 15.0                       | 10.3    |
| digit            | 122             | 435         | 152.5                      | 12                    | 58.8            | 14.9                       | 10.2    |
| hist             | 97              | 45          | 121.2                      | 9                     | 17.1            | 11.3                       | 10.8    |
| sc               | 104             | 145         | 130.0                      | 10                    | 27.9            | 12.4                       | 10.4    |
| select           | 106             | 145         | 132.5                      | 10                    | 27.6            | 12.5                       | 10.6    |

<sup>7</sup>The cost is estimated based on an enterprise online cost estimator [62], using a public-cloud system with configuration akin to our on-prem system. Specifically, we have selected an *n2* (8-core, 64GB RAM VM - 1.25\$/h) for bitstream generation (x86) and an *np87l* instance (160-thread POWER8, 1TB RAM, ADM-PCIE-KU3 with CAP1-1 - 3\$/h) for deployment.

effective speedup compared to a traditional “brute-force” approach.

In Table VII, we mention the performance and resource utilization for our considered applications both on a low-end system and a high-end cloud system. We use LEAPER, to obtain the performance and resource utilization for the high-end cloud configuration.

#### D. Base Model Accuracy Analysis

We also evaluate the accuracy of our base model. The base model (Section II-C) is trained on our low-end edge PYNQ board using  $c_{lhs}$  configurations sampled using DoE technique. The base can predict performance (or resource utilization) outside the base learner dataset (i.e., any configuration that is not a part of the DoE configuration space)  $c_{lhs}$  (ref. Figure 2). To assess our base model, we use 30 previously unseen configurations that are not part of  $c_{lhs}$  on the base system, and we evaluate the mean relative error for all 30 unseen configurations on all six applications. Figure 7 shows LEAPER’s base model accuracy results. We also compare LEAPER to three other ML algorithms that are also trained using  $c_{lhs}$  configurations to predict performance and resource consumption: XG-Boost (XGB) [63] based on Dai *et al.* [21],

**TABLE VII:** Execution time and resource utilization for low-end base configuration (PYNQ-Z1) and high-end cloud configuration, a Nimbix *np8fl* instance.

| Application | Config.  | Exec (msec) | BRAM | DSP  | FF  | LUT |
|-------------|----------|-------------|------|------|-----|-----|
| blstm       | low-end  | 4200        | 80%  | 15%  | 24% | 47% |
|             | high-end | 1245        | 62%  | 8%   | 12% | 21% |
| cedd        | low-end  | 10254       | 83%  | 37%  | 95% | 97% |
|             | high-end | 2217        | 56%  | 3%   | 75% | 94% |
| digit       | low-end  | 2458        | 94%  | 33%  | 79% | 85% |
|             | high-end | 873         | 84%  | 12%  | 24% | 75% |
| hist        | low-end  | 6173        | 94%  | 0%   | 11% | 37% |
|             | high-end | 1104        | 67%  | 0%   | 5%  | 30% |
| sc          | low-end  | 19306       | 82%  | 0.4% | 12% | 25% |
|             | high-end | 4018        | 91%  | 0.1% | 12% | 23% |
| select      | low-end  | 18306       | 82%  | 0.4% | 12% | 25% |
|             | high-end | 3918        | 91%  | 0.1% | 12% | 23% |

an artificial neural network (ANN) used by Makrani *et al.* [20] and a traditional decision tree (DT). We make three observations. First, on average, LEAPER is more accurate in terms of performance (resource utilization) prediction than the other ML models. Second, XGBoost is more data-efficient than ANNs [21] and can perform better than decision trees [64]. Third, ANN is more accurate than the decision tree, but it is less accurate than LEAPER. This is because ANN requires a much larger training dataset to reach LEAPER’s accuracy [65].

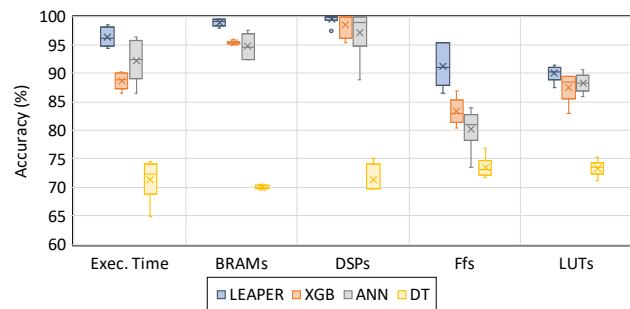


**Fig. 7:** Mean accuracy for performance and resource utilization predictions using LEAPER’s base model and other popular machine learning techniques.

### E. Why does LEAPER work?

To explain our results for transfer learning, we analyze the degree of *relatedness* between the source and target environments. We perform Pearson correlation analysis [66] followed by a divergence analysis [67] of the performance distributions of the environments.

Using the correlation analysis, we make the following three observations. First, for different target hardware platforms, we see a high correlation of 0.76 to 0.97 between the source and target execution time, which indicates that the target model’s performance behavior can easily be learned using the source environment. As the linear correlation is not 1 for all platforms, the use of a nonlinear transfer model is substantiated. Second, as we switch to a higher external bandwidth for the target platform (i.e., CAPI1 to CAPI2), the correlation becomes lower because the hardware change is much more *severe* coming from a low-end FPGA with limited external bandwidth. Third, the correlation between applications on a single platform is lower (0.45 to 0.9) because of the varying application characteristics and optimization space.

We measure the relatedness of the performance distributions of the source ( $P(\tau_s)$ ) and the target applications ( $P(\tau_t)$ ). This analysis measures the degree of non-linearity because application-based environments exhibit a low linear correlation. We employ the Jensen-Shannon Divergence (JSD) [68] (*ref.* Table VIII) to quantify the statistical distance between  $P(\tau_s)$  and  $P(\tau_t)$ . The lower the values of JSD, the more similar the target environment

**TABLE VIII:** Jensen-Shannon Divergence (JSD) [68] between performance distributions of different applications. JSD measures statistical distance between two probability distributions.

|              |        | Base Learner |      |       |      |      |        |
|--------------|--------|--------------|------|-------|------|------|--------|
|              |        | blstm        | cedd | digit | hist | sc   | select |
| Target Model | blstm  | 0.00         | 0.24 | 0.34  | 0.25 | 0.31 | 0.30   |
|              | cedd   | 0.24         | 0.00 | 0.49  | 0.54 | 0.41 | 0.40   |
|              | digit  | 0.34         | 0.49 | 0.00  | 0.25 | 0.21 | 0.21   |
|              | hist   | 0.25         | 0.54 | 0.25  | 0.00 | 0.25 | 0.24   |
|              | sc     | 0.30         | 0.40 | 0.21  | 0.24 | 0.00 | 0.05   |
|              | select | 0.30         | 0.41 | 0.21  | 0.25 | 0.05 | 0.00   |

is to the source (i.e., if  $D_{JSD}(P(\tau_t)||P(\tau_s)) = 0$  implies the distributions are identical and 1 indicates unrelated distributions). This analysis confirms the trend observed from transferring application models (Figure 5), i.e., the more closely related the source and target applications, the fewer samples are required to train our non-linear transfer learners. The measured distance between the tasks is proportional to the error of the target task. As can be seen from Table VIII for many applications, transfer learning to build accurate models is feasible since their JSD is limited. Similar trends are observed for the resource utilization model.

### F. Discussion and Limitations

**Transfer to a new platform and application simultaneously.** In supervised learning, transferring both to a new platform and application at the same time would lead to sub-optimal results (as observed in [69]) this is because we would perform two-levels of transfer. Moreover, for transfer learning, an ML model needs to have some notion of the target environment. Therefore, we explicitly exclude this option in the paper.

**FPGA resource constrained environments.** During partial reconfiguration [70] or in a multi-tenant environment [5], we are often constrained by limited resources [71]. In such scenarios, the resource management is more efficient to be controlled by a middleware layer [72]. We do not assume such as a middleware. Therefore, our analysis targets bare-metal systems. In future, we aim to extend our work to such scenarios as well.

**LEAPER generality to other platforms.** LEAPER, in essence, is a framework for building and then transferring models from a small edge platform to any new, unknown FPGA-based environment. We demonstrate our approach using the cloud as our target environment because cloud systems often use expensive, high-end FPGAs, e.g., Amazon AWS F1 cloud [3], Alibaba Elastic cloud with FPGAs [4], etc. We can, thus, achieve tangible gains in terms of cost, efficiency, and performance.

**Effect of FPGA resource saturation.** An FPGA gives us the flexibility to map operation to different resources. For example, we can map a multiplication operation either to a CLB or a DSP slice. The deciding factor is the operand width. If the operand width is smaller than DSP slice width, the operation is mapped to a CLB else to a DSP unit. An ML-model can be trained to learn such relations. However, we avoid it in our current work.

## IV. RELATED WORK

To our knowledge, this is the first paper to propose the transfer of FPGA-based performance (resource) models. FPGAs are infamous for low productivity due to the time-consuming downstream implementation process. We have extensively evaluated our approach using five FPGA-based platforms with three different interconnect technologies on six real-world applications. In this section, we describe other related works in FPGA ML-based modeling, analytical modeling, and transfer learning.

**FPGA ML-Based Modeling.** Recent works propose ML-based methods [16]–[25] to overcome the issue of low productivity with FPGAs. O’Neal *et al.* [16] uses CPU

performance counters to train several ML-based models to predict FPGA performance and power consumption. Makrani *et al.* [20] trained a neural network-based model to predict application speedup across different FPGAs. Makrani *et al.* [17] and Dai *et al.* [21] use ML to predict resource utilization for an FPGA implementation. However, these solutions become largely impractical once the platform, the application, or even the size of the workload changes. LEAPER proposes to reuse previously built models on a low-end source environment to accelerate the learning of ML models on a high-end target environment through transfer learning. Unlike LEAPER, past works apply traditional, time-consuming brute-force techniques to collect training dataset. These techniques quickly become intractable when the number of optimization parameters increases due to the curse of dimensionality [73].

**Transfer Learning.** Recently, transfer learning [27], [74], [75] has gained traction to decrease the cost of learning by transferring knowledge. Valov *et al.* [76] investigated the transfer of application models across different CPU-based environments using linear transformations. Jamshidi *et al.* [41] demonstrated the applicability of using nonlinear models to transfer CPU-based performance models. The works above influenced the design of LEAPER. In contrast, we: (1) focus on FPGA-based systems that, unlike a CPU-based system, has a different hardware architecture for every application and optimization strategy, and (2) use an ensemble of transfer learners that transfers accurate models to a target environment.

## V. CONCLUSION

We introduce LEAPER, the first *transfer learning*-based approach to transfer FPGA-based prediction models. LEAPER combines statistical techniques and transfer learning to minimize the ML training data collection overhead. It overcomes the inefficiency of traditional ML-based methods by accurately *transferring* an existing ML model built on an inexpensive, low-end FPGA platform to a new, unknown, high-end environment.

Our experiments show that we can develop cheaper (with *5-shot*), faster (up to 10 $\times$ ), and highly accurate (on average 85%) models to predict performance and resource consumption in a new, unknown target cloud environment. We believe that LEAPER would open up new avenues for research on FPGA-based systems from edge to cloud computing, and hopefully, inspires the development of new modeling techniques.

## REFERENCES

- [1] A. Putnam *et al.*, "A reconfigurable fabric for accelerating large-scale datacenter services," in *ISCA*, 2014.
- [2] Y.-K. Choi *et al.*, "In-depth analysis on microarchitectures of modern heterogeneous cpu-fpga platforms," *TRETS*, 2019.
- [3] "Amazon Web Services. AWS FPGA Developer AMI, <https://aws.amazon.com/ec2/instance-types/f1>, Accessed: 2020-06-10."
- [4] "Alibaba cloud, [www.alibabacloud.com](http://www.alibabacloud.com), Accessed: 2020-06-10."
- [5] A. Pourhabibi *et al.*, "Optimus prime: Accelerating data transformation in servers," in *ASPLOS*, 2020.
- [6] S. Byma *et al.*, "Fpgas in the cloud: Booting virtualized hardware accelerators with openstack," in *FCCM*, 2014.
- [7] G. Singh, D. Diamantopoulos, C. Hagleitner, J. Gomez-Luna, S. Stuijk, O. Mutlu, and H. Corporaal, "NERO: A Near High-Bandwidth Memory Stencil Accelerator for Weather Prediction Modeling," in *FPL*, 2020.
- [8] G. Singh, D. Diamantopoulos, S. Stuijk, C. Hagleitner, and H. Corporaal, "Low Precision Processing for High Order Stencil Computations," in *Springer LNCS*, 2019.
- [9] G. Singh *et al.*, "NARMADA: Near-Memory Horizontal Diffusion Accelerator for Scalable Stencil Computations," in *FPL*, 2019.
- [10] G. Singh, M. Alser, D. S. Cali, D. Diamantopoulos, J. Gómez-Luna, H. Corporaal, and O. Mutlu, "FPGA-based Near-Memory Acceleration of Modern Data-Intensive Applications," *IEEE Micro*, 2021.
- [11] G. Singh, D. Diamantopoulos, J. Gómez-Luna, C. Hagleitner, S. Stuijk, H. Corporaal, and O. Mutlu, "Accelerating weather prediction using near-memory reconfigurable fabric," *TRETS*, 2022.
- [12] J. van Lunteren, R. Luijten, D. Diamantopoulos, F. Auernhammer, C. Hagleitner, L. Chelini, S. Corda, and G. Singh, "Coherently Attached Programmable Near-Memory Acceleration Platform and its application to Stencil Processing," in *DATE*, 2019.
- [13] D. Diamantopoulos, B. Ringlein, M. Purandare, G. Singh, and C. Hagleitner, "Agile autotuning of a transprecision tensor accelerator overlay for tvn compiler stack," in *FPL*, 2020.
- [14] G. Singh, D. Diamantopoulos, J. Gómez-Luna, S. Stuijk, O. Mutlu, and H. Corporaal, "Modeling fpga-based systems via few-shot learning," in *FPGA*, 2021.
- [15] K. O'Neal and P. Brisk, "Predictive modeling for cpu, gpu, and fpga performance and power consumption: A survey," in *VLSI*, 2018.
- [16] K. O'Neal *et al.*, "HLSPredict: Cross Platform Performance Prediction for FPGA High-Level Synthesis," in *ICCAD*, 2018.
- [17] H. M. Makrani *et al.*, "Pyramid: Machine learning framework to estimate the optimal timing and resource usage of a high-level synthesis design," in *FPL*, 2019.
- [18] M. Ferianc *et al.*, "Improving performance estimation for fpga-based accelerators for convolutional neural networks," in *ARC*, 2020.
- [19] E. Ustun *et al.*, "Accurate operation delay prediction for fpga hls using graph neural networks," in *ICCAD*, 2020.
- [20] H. M. Makrani *et al.*, "XPPE: Cross-Platform Performance Estimation of Hardware Accelerators Using Machine Learning," in *ASP-DAC*, 2019.
- [21] S. Dai *et al.*, "Fast and Accurate Estimation of Quality of Results in High-Level Synthesis with Machine Learning," in *FCCM*, 2018.
- [22] J. Zhao, T. Liang, S. Sinha, and W. Zhang, "Machine learning based routing congestion prediction in fpga high-level synthesis," in *DATE*, 2019.
- [23] Q. Yanghua, N. Kapre, H. Ng, and K. Teo, "Improving classification accuracy of a machine learning approach for fpga timing closure," in *FCCM*, 2016.
- [24] Z. Wang and B. C. Schafer, "Machine learning to set meta-heuristic specific parameters for high-level synthesis design space exploration," in *DAC*, 2020.
- [25] A. Mahapatra and B. C. Schafer, "Machine-learning based simulated annealer method for high level synthesis design space exploration," in *ESLsyn*, 2014.
- [26] W. Dai, Q. Yang, G.-R. Xue, and Y. Yu, "Boosting for transfer learning," in *ICML*, 2007.
- [27] S. J. Pan and Q. Yang, "A survey on transfer learning," *IEEE TKDE*, 2009.
- [28] Y. Wang and Q. Yao, "Few-shot learning: A survey," *CoRR*, 2019. [Online]. Available: <http://arxiv.org/abs/1904.05046>
- [29] P. H. Swain and H. Hauska, "The decision tree classifier: Design and potential," *IEEE GE*, 1977.
- [30] L. Breiman, "Random forests," *Machine learning*, 2001.
- [31] D. C. Montgomery, *Design and analysis of experiments*. John Wiley & sons, 2017.
- [32] D. Ópitz and R. Maclin, "Popular ensemble methods: An empirical study," *JAIR*, 1999.
- [33] "Vivado High-Level Synthesis, <https://www.xilinx.com/products/design-tools/vivado/integration/esl-design.html>."
- [34] "Vivado Design Suite User Guide High-Level Synthesis, [https://www.xilinx.com/support/documentation/sw\\_manuals/](https://www.xilinx.com/support/documentation/sw_manuals/)."
- [35] A. Anghele *et al.*, "An instrumentation approach for hardware-agnostic software characterization," *IJPP*, 2016.
- [36] L. Breiman, "Bagging predictors," *ML*, 1996.
- [37] G. Mariani *et al.*, "Predicting cloud performance for HPC Applications: A user-oriented approach," in *CCGRID*, 2017.
- [38] J. H. Friedman, "Greedy function approximation: a gradient boosting machine," *Annals of statistics*, 2001.
- [39] R. E. Schapire, "The strength of weak learnability," *ML*, 1990.
- [40] S. Kotsiantis and P. Pintelas, "Combining bagging and boosting," *IJCS*, 2004.
- [41] P. Jamshidi *et al.*, "Transfer Learning for Improving Model Predictions in Highly Configurable Software," in *SEAMS*, 2017.
- [42] C. E. Rasmussen, "Gaussian processes in machine learning," in *Summer School on Machine Learning*. Springer, 2003.
- [43] J. Gómez-Luna *et al.*, "Chai: Collaborative Heterogeneous Applications for Integrated-architectures," in *ISPASS*, 2017.
- [44] D. Diamantopoulos *et al.*, "eCTALK: Energy efficient coherent transprecision accelerators—the bidirectional long short-term memory neural network case," in *COOL CHIPS*, 2018.
- [45] Y. Zhou *et al.*, "Rosetta: A realistic high-level synthesis benchmark suite for software programmable FPGAs," in *FPGA*, 2018.
- [46] J. Gómez-Luna *et al.*, "In-place data sliding algorithms for many-core architectures," in *ICPP*, 2015.
- [47] M. R. Yousefi *et al.*, "Binarization-free ocr for historical documents using LSTM networks," in *ICDAR*, 2015.
- [48] "PYNQ-Z1: Python Productivity for Zynq-7000 ARM/FPGA SoC, <https://www.xilinx.com/products/boards-and-kits/1-hydd4z.html>."
- [49] "Accelerator Coherency Port, Cortex-A9 MPCore Technical Reference Manual, Arm Ltd., <https://developer.arm.com/documentation/ddi0407/e/snoop-control-unit/accelerator-coherency-port>."
- [50] "Openstack, <https://www.openstack.org>, Accessed: 2020-06-12."
- [51] "ADM-PCIE-8K5-High-Performance Data Processing, <https://www.alpha-data.com/dcp/products.php?product=adm-pcie-8k5>."
- [52] "ADM-PCIE-KU3-High-Performance Data Processing, <https://www.alpha-data.com/dcp/products.php?product=adm-pcie-ku3>."
- [53] "NSA.241 FPGA accelerator card, <http://www.semptian.com/product/info/126.html>."
- [54] "ADM-PCIE-9V3-High-Performance Network Accelerator, <https://www.alpha-data.com/dcp/products.php?product=adm-pcie-9v3>."
- [55] "Nallatech 250SP, <http://www.nallatech.com/250sp>."
- [56] "SDSoc Development environment, <https://www.xilinx.com/products/design-tools/software-zone/sdsoe.html>."
- [57] A. Castellane and B. Mesnet, "Enabling fast and highly effective fpga design process using the capi snap framework," in *ISC HPC*, 2019.

- [58] “AXI Reference Guide, [https://www.xilinx.com/support/documentation/ip\\_documentation/ug761\\_axi\\_reference\\_guide.pdf](https://www.xilinx.com/support/documentation/ip_documentation/ug761_axi_reference_guide.pdf).”
- [59] W.-Y. Loh, “Classification and regression trees,” *WIREs Data Mining and Knowledge Discovery*, 2011.
- [60] Y. Freund and R. E. Schapire, “A decision-theoretic generalization of on-line learning and an application to boosting,” *JCSS*, 1997.
- [61] “Vivado 2020.2 Developer AMI, <https://aws.amazon.com/marketplace/pp/xilinx-vivado-20202-developer-ami/b08pvvmhmq>, Accessed: 2021-02-01.”
- [62] “Nimbix Cloud Price Calculator, <https://www.nimbix.net/cloud-price-calculator>, Accessed: 2020-06-13.”
- [63] T. Chen and C. Guestrin, “XGBoost: A Scalable Tree Boosting System,” in *SIGKDD*, 2016.
- [64] G. Singh *et al.*, “NAPEL: Near-Memory Computing Application Performance Prediction via Ensemble Learning,” in *DAC*, 2019.
- [65] D. Li *et al.*, “Processor design space exploration via statistical sampling and semi-supervised ensemble learning,” *IEEE Access*, 2018.
- [66] J. Benesty, J. Chen, Y. Huang, and I. Cohen, “Pearson correlation coefficient,” in *Noise reduction in speech processing*. Springer, 2009, pp. 1–4.
- [67] B. Coutinho, D. Sampaio, F. M. Q. Pereira, and W. Meira Jr, “Divergence analysis and optimizations,” in *PACT*, 2011.
- [68] J. Lin, “Divergence measures based on the Shannon entropy,” *IEEE Trans. Inf. Theory*, 1991.
- [69] N. Ardalani *et al.*, “Cross-architecture performance prediction (XAPP) using CPU code to predict GPU performance,” *ISCA*, 2015.
- [70] C. Beckhoff, D. Koch, and J. Torresen, “Go ahead: A partial reconfiguration framework,” in *FCCM*, 2012.
- [71] H.-Y. Ting *et al.*, “Dynamic sharing in multi-accelerators of neural networks on an fpga edge device,” in *ASAP*, 2020.
- [72] A. Vaishnav *et al.*, “Fos: A modular fpga operating system for dynamic workloads,” *arXiv preprint*, 2020.
- [73] R. Bellman, “Dynamic programming,” *Science*, 1966.
- [74] H. Chen *et al.*, “Experience transfer for the configuration tuning in large-scale computing systems,” *IEEE TKDE*, 2010.
- [75] U. Baumann *et al.*, “Classifying road intersections using transfer-learning on a deep neural network,” in *ITSC*, 2018.
- [76] P. Valov *et al.*, “Transferring Performance Prediction Models Across Different Hardware Platforms,” in *ICPE*, 2017.